Catalysis Today 178 (2011) 124–131

Contents lists available at SciVerse ScienceDirect

Catalysis Today

journal homepage: www.elsevier.com/locate/cattod

Redox properties of supported copper catalysts studied in liquid and gas phase by *in situ* ATR-IR and XAS

Cecilia Mondelli[a], Davide Ferri[b], Jan-Dierk Grunwaldt[c], Nicoletta Ravasio[d], Alfons Baiker[a,e,*]

[a] Institute for Chemical and Bioengineering, Department of Chemistry and Applied Biosciences, ETH Zurich, Hönggerberg, Wolfgang-Pauli-Str. 10, CH-8093 Zürich, Switzerland
[b] Empa, Swiss Federal Laboratories for Material Science and Technology, Laboratory for Solid State Chemistry and Catalysis, Ueberlandstrasse 129, CH-8600 Dübendorf, Switzerland
[c] Institute for Chemical Technology and Polymer Chemistry, Karlsruhe Institute of Technology (KIT), Engesserstr. 20, D-76131 Karlsruhe, Germany
[d] CNR, Institute of Molecular Science and Technologies, via Golgi 19, I-20133 Milan, Italy
[e] Chemistry Department, Faculty of Science, King Abdulaziz University, P.O. Box 80203, Jeddah 21589, Saudi Arabia

ARTICLE INFO

Article history:
Received 30 July 2011
Received in revised form 25 August 2011
Accepted 27 August 2011
Available online 1 October 2011

Keywords:
Supported copper catalysts
Redox properties
In situ ATR-IR
In situ X-ray absorption spectroscopy
Support effect
Liquid phase
Gas phase
Anaerobic alcohol oxidation

ABSTRACT

The redox behavior of copper-based catalysts plays a prominent role in several important chemical processes. So far relatively little is known about how this behavior is affected by the medium (liquid or gas phase) in which the copper particles are immersed. In this study, we have investigated the redox properties of copper nanoparticles supported on Al_2O_3, TiO_2 and SiO_2 in the liquid (presence of solvent) and gas phase by means of *in situ* Attenuated Total Reflection Infrared spectroscopy (ATR-IR) and *in situ* X-ray absorption spectroscopy (XAS) in combination with CO adsorption. Using CO and H_2 as a reducing agent, the presence of the solvent was found to facilitate reduction of the copper constituent at lower temperatures than in the gas phase. Furthermore, the nature of the support strongly affected the extent of the reduction of the copper constituent. Copper was spontaneously reduced in the presence of CO-saturated solvent to an extent increasing in the order $Cu/SiO_2 < Cu/Al_2O_3 < Cu/TiO_2$. In the gas phase, reduction of the copper constituent in Cu/Al_2O_3 was more difficult than that in Cu/SiO_2. The reduction behavior measured in the presence of the solvent was found to be correlated to the activity of the catalysts in the anaerobic oxidation of 3-octanol.

1. Introduction

Supported metal particles play a key role in heterogeneous catalysis. The majority of the catalytic processes is based on the unique features of surface metallic aggregates, which interact with reactant molecules, thus favoring bond scission and formation. The nano-character of supported metal particles confers peculiar electronic and geometric properties that often account for improved catalytic performances. Therefore, many efforts have been undertaken in the past years to discover innovative synthetic routes, leading to finely dispersed nanoparticles [1–4]. The electronic properties of the metal experience strong variation in the transition from the continuous energy band in the bulk metal to the discrete energy levels of the isolated surface atoms. This may for instance reflect in modified redox properties. Additionally, it has been very often observed that catalytic performances and stability of the metal-based catalysts are strongly dependent, for example, on the nature of the support, on the preparation method, and on the activation procedure of the material [5–10]. It is therefore important to determine the oxidation state of the metal at the different stages of its use, since this factor critically influences its catalytic performance.

Among the wide variety of metals successfully employed in catalytic oxidation or reduction reactions, copper plays a prominent role. Methanol synthesis, steam reforming, oxychlorination and selective reduction of NO constitute important applications of copper catalysts in gas-phase processes [11–17]. Copper dispersion and morphology has been shown to be one of the key factors influencing the catalytic activity in these reactions [18–21]. Prominent copper-catalyzed liquid-phase reactions include both selective hydrogenations of carbonyl compounds and oxidation of alcohols [22–31], as well as hydrogenolysis of esters [32], and amination of alcohols [33], just to name a few. The requirement of reductive pretreatments prior to application of these catalysts has proven to be crucial for the majority of catalyzed redox processes occurring in liquid phase, because oxidized Cu species can be totally inactive. Supported nano-sized copper particles prepared by a chemisorption-hydrolysis method [34] have recently been shown to possess remarkable activity in the anaerobic oxidation of non-activated alcohols [35,36]. Still, appreciable differences in performance have been observed depending on the type of support employed.

* Corresponding author at: Institute for Chemical and Bioengineering, Department of Chemistry and Applied Biosciences, ETH Zurich, Hönggerberg, Wolfgang-Pauli-Str. 10, CH-8093 Zürich, Switzerland. Fax: +41 44 632 11 63.
E-mail address: baiker@chem.ethz.ch (A. Baiker).

0920-5861/$ – see front matter © 2011 Elsevier B.V. All rights reserved.
doi:10.1016/j.cattod.2011.08.043

Here we have investigated the redox properties of differently supported copper catalysts (Cu/Al_2O_3, Cu/TiO_2, Cu/SiO_2) in the liquid and gas phase. In the center of our interest was the reducibility of the copper constituent and how it is affected by the presence of a solvent and the nature of the support. Despite a clear need for investigating the properties of catalysts under conditions relevant to their catalytic applications, characterization in liquid media has been mainly confined to Pd-, Pt-, Au- and Ru-based catalysts so far [37–46]. Only a very limited number of studies has been dedicated to the chemistry of copper-based systems under *in situ* conditions [47–50]. Two established powerful techniques for studying heterogeneous catalysts at a molecular level have been applied in this work. *In situ* Attenuated Total Reflection Infrared spectroscopy (ATR-IR) combined with CO adsorption enabled defining the electronic properties of the binding metal sites and the surface morphology of the copper nanoparticles in the liquid environment. *In situ* X-ray absorption spectroscopy (XAS) allowed shedding light on the changes of the oxidation state and structure of the copper phase immersed in the liquid medium. Parallel characterization by DRIFTS and XAS in a more conventional gas-phase approach was conducted to highlight the advantages of the *in situ* methods.

2. Materials and methods

2.1. Materials

The 8 wt.% Cu/Al_2O_3, Cu/TiO_2 and Cu/SiO_2 catalysts have been prepared by the chemisorption-hydrolysis technique described elsewhere [34]. Solvents (*n*-heptane, toluene and ethanol, >98%) were used as received. Gases (H_2, CO, O_2 and Ar, 99.999 vol.%; 10 vol.% CO/Ar and 5 vol.% H_2/He) were purchased from PANGAS.

2.2. ATR-IR spectroscopy

Particulate films were deposited on the trapezoidal ZnSe internal reflection element (IRE, 45°, 52 mm × 20 mm × 2 mm, Komlas) by dropping on its larger side aqueous slurries of the materials, as previously described [39]. The amount of deposited catalyst was about 4 mg. ATR-IR measurements have been carried out using a stainless steel home-made flow-through reactor cell [51] mounted on the optical bench of an Equinox 55 (Bruker Optics, Germany) infrared spectrometer equipped with a MCT detector cooled with liquid nitrogen. Heptane solvent saturated with H_2, CO and O_2 was provided from three separated glass bubble reservoirs and connected to the inlet of the ATR cell by means of a pneumatically activated Teflon valve. Liquids were admitted at a rate of 0.65 ml/min using a peristaltic pump (ISMATEC, Reglo 100) located downstream the cell. Stainless steel tubing was used throughout. The temperature of the cell was controlled with a water thermostat. The following protocol was used in CO adsorption experiments. After deposition on the ZnSe IRE, the Cu/Al_2O_3 film was reduced *ex situ* under H_2 flow for 1 h at 453 K (denoted as "pre-reduced" catalyst). After cooling to room temperature in hydrogen flow, the coated IRE was quickly (<5 min) transferred to the spectroscopic cell. Prolonged exposure to air resulted in complete reoxidation of the material. Once the IRE was mounted in the cell, the film was immediately contacted with H_2-saturated heptane for 60 min at 353 K. Then a CO (120 min)–O_2 (20 min)–CO (120 min) cycle followed. CO adsorption experiments were performed at 283, 313 and 353 K. Identical experiments were repeated for the unreduced catalyst. In order to determine the effect of the support phase, CO adsorption was also carried out on the *ex situ* pre-reduced Cu/TiO_2 and Cu/SiO_2 at 353 K only. ATR-IR spectra were collected (4000–800 cm^{-1}) by averaging 200 scans at 4 cm^{-1} resolution. The spectra are presented in absorbance units, where the last spectrum obtained during *in situ* reduction of the catalyst is used as the reference. Where required, spectra were corrected to compensate for the absorption of atmospheric water.

2.3. DRIFT spectroscopy

Diffuse reflectance measurements were performed using an EQUINOX 55 spectrometer (Bruker Optics) equipped with a HVC-DRP2 reaction chamber (Harrick) and a MCT detector cooled with liquid nitrogen. All Cu-based catalysts (10 mg) were diluted with KBr. CO adsorption was performed at 353 K under dynamic conditions after reduction at 353 K in flowing H_2 for 1 h. Identical experiments were repeated after reduction at 453 K. The gas-flow rate was set at 10 ml/min. Spectra are reported in Kubelka-Munk units without further correction.

2.4. X-ray absorption spectroscopy

The *in situ* X-ray absorption spectroscopy measurements were carried out both in gas and liquid phase [52,53] at the XAS beam line of the ANKA synchrotron radiation facility (Karlsruhe Institute of Technology, Germany) in the transmission geometry using a Si(1 1 1) double crystal for monochromatization of the beam at the Cu K-edge (8.979 keV). By detuning the crystals to 70% of the maximum intensity, higher harmonics were effectively eliminated. Three ionization chambers filled with N_2 were used to record the intensity of the incident and the transmitted X-rays. The cell was located between the first and second chamber. A Cu reference foil for energy calibration was placed between the second and the third ionization chamber. Under stationary conditions EXAFS spectra were taken around the Cu K-edge in the step scanning mode between 8.830 and 9.950 keV. During dynamic changes (temperature, gas atmosphere) quick EXAFS (QEXAFS) scans were recorded in the continuous scanning mode between 8.900 and 9.200 keV (typically 70 s/scan). For the analysis of EXAFS data, Fourier transformation was applied on the k^1-weighted functions in the interval k = 2.6–14 $Å^{-1}$ using the WINXAS 3.1 software [54]. The reactor cell with 2 mm penetration length was filled with about 15 mg of the corresponding Cu-based catalysts and fixed on an x, z, θ table to allow positioning of the cell in the beam. The X-rays passed through the reactor cell via X-ray transmitting windows. The experimental setup consisted of two independent stainless steel lines connected by means of a three-way valve before the reactor to allow admission of a feed from either way. One line was connected to the gas bottles (for gas phase treatments) and one to similar equipment to that previously described for liquid phase ATR-IR studies (for liquid-phase treatments). In particular, a glass bubble reservoir contained neat solvent saturated with H_2. The second and third reservoirs contained CO-saturated and O_2-saturated solvent, respectively. Liquids were provided to the reactor by a peristaltic pump (ISMATECReglo 100) set in front of the reactor. The flow rate was 0.65 ml/min. The experimental procedure resembled that employed for the ATR-IR measurements. Samples were reduced under H_2 flow (5 vol.% in He) at 543 K (453 K for Cu/TiO_2) for 1 h and then cooled under Ar to 353 K. Before admitting the liquid phase to the catalyst, the lines were disconnected for a short while in order to allow diffusion of air, in this way simulating the transfer of the coated IRE to the ATR-IR cell. CO adsorption was then performed from CO (10 vol.% in Ar)-saturated solvent. O_2-saturated solvent was afterwards admitted to the cell. Finally, the catalyst was again exposed to CO (10 vol.% in Ar)-saturated heptane.

2.5. Catalytic testing

The catalysts (0.1 g) were treated at 413 K for 20 min in air, 20 min under reduced pressure and 20 min under H_2 in a glass

reactor. 3-Octanol (0.1 g) was dissolved in toluene (8 ml, as received) and the solution transferred under N_2 into the reaction vessel. Dehydrogenation of the alcohol was carried out at 363 K under N_2 and magnetic stirring for 30 min. Conversion to the carbonyl product was determined by GC using a crosslinked 5% phenyl methyl silicone (HP-5MS, 30 m) capillary column.

3. Results

3.1. Basic characterization

As specified in Section 2, the copper loading in Cu/Al_2O_3, Cu/TiO_2 and Cu/SiO_2 was 8 wt.%. The surface area of the exposed copper, as determined by N_2O chemisorption for the three catalysts, was 49, 55, and 129 $m^2\,g_{Cu}^{-1}$, respectively [55,56]. In all cases CO chemisorption from the gas phase has shown the presence of three dimensional metallic Cu nanoparticles with uniform and well-defined distribution of surface sites, mainly made up of low index faces [55–57]. The copper particle sizes in the differently supported copper catalysts, as determined by TEM, were: 4–6 nm for Cu/Al_2O_3, 4–6 nm for Cu/TiO_2, and 3–4 nm for Cu/SiO_2. Temperature programmed reduction (TPR) with H_2 indicated that the reduction temperature of supported copper increased in the order Cu/TiO_2 (457 K) < Cu/Al_2O_3 (483 K) < Cu/SiO_2 (495 K) [29,36,55]. The reduction profile of Cu/TiO_2 exhibited three reduction peaks, suggesting a stronger interaction between some copper species and lattice O atoms of the support.

3.2. ATR-IR

Fig. 1 shows the ATR-IR spectra obtained after CO adsorption from CO-saturated heptane at 283, 313 and 353 K, on *ex situ* pre-reduced (453 K) and unreduced Cu/Al_2O_3. Given the fast re-oxidation of Cu after exposure to air, the samples were further reduced *in situ* with H_2-saturated solvent prior to CO adsorption at 353 K. A broad feature (2110–2080 cm^{-1}) likely composed of two overlapping signals was observed for pre-reduced Cu/Al_2O_3 at 353 K in the spectral range related to CO adsorption in linear geometry on metallic Cu, as known from gas-phase experiments (Fig. 1a) [55,56,58–62]. The presence of the high frequency component indicates that copper species in partially oxidized state may exist, although Cu(I) carbonyls are known to be stable surface species under oxidizing conditions. The signal with a maximum at 2091 cm^{-1} on the catalyst reduced at 313 K is less pronounced and is red-shifted with respect to the signal observed at 353 K (2099 cm^{-1}), indicating a lower degree of Cu reduction. The pattern shows a more asymmetric signal with a more pronounced shoulder at higher energy. The signal obtained during adsorption at 283 K was negligible. The spectrum obtained for the unreduced catalyst at 353 K resembles that measured at 313 K for the reduced Cu/Al_2O_3 (Fig. 1b). No significant adsorptions were observed at 313 and 283 K.

Fast and complete signal depletion occurred after admission of O_2-saturated solvent on both pre-reduced and unreduced Cu/Al_2O_3. Changing the liquid flow back to CO-saturated solvent only partially restored the signal intensity. Furthermore, despite the overall signal intensity was lower, the shape of the signal remained unchanged, but the CO adsorption kinetics appeared slower. Representative ATR-IR spectra of pre-reduced Cu/Al_2O_3 during the CO–O_2–CO cycle, along with the CO adsorption profiles in the two phases, are presented as Supplementary Material (Fig. S1).

The ATR-IR studies suggest that copper was mainly present in the oxidic state during the treatment with CO. However, spontaneous reduction of copper appeared to take place *in situ* when the catalyst was exposed to CO-saturated heptane. The starting

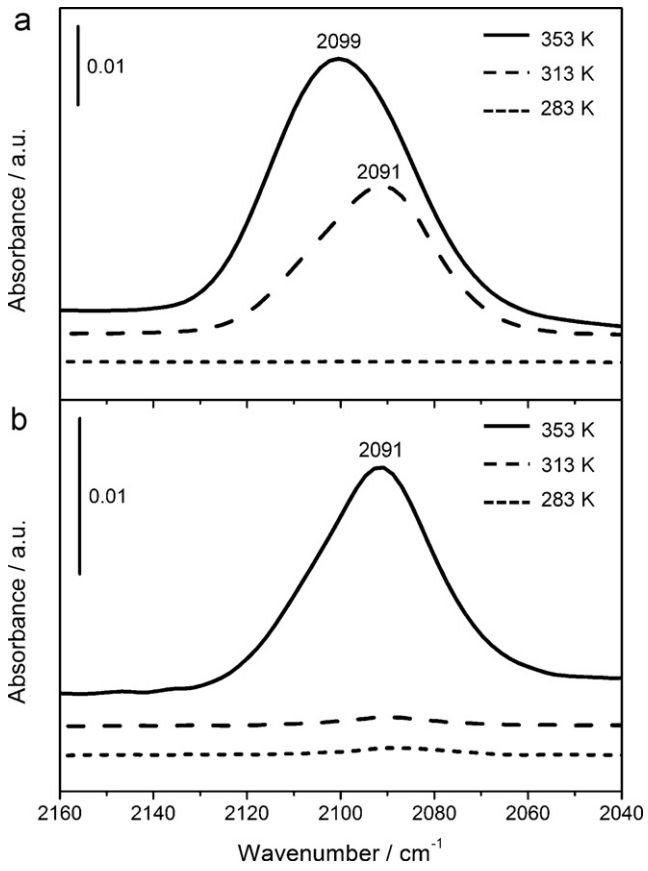

Fig. 1. ATR-IR spectra of CO adsorbed on pre-reduced (a) and unreduced (b) Cu/Al_2O_3. Conditions: heptane solvent, CO, 2 h. Pre-reduction: 453 K. *In situ* reduction: 353 K.

oxidation state of the sample and the temperature significantly affected the extent of copper reduction by CO, its consequent adsorption and the relative distribution of Cu(0) and Cu(I) species. Thus, no metallic copper phase was formed if the original sample was in non pre-reduced (extensively oxidized) form and/or a low adsorption temperature was employed.

The effect of the nature of the support on the electronic properties of copper was explored by comparing the reducibility of copper species during CO adsorption experiments with Cu/Al_2O_3, Cu/TiO_2 and Cu/SiO_2. The ATR-IR spectra collected at 353 K for the three catalysts are depicted in Fig. 2. Comparison of these spectra in terms of intensity and symmetry of the signal associated with the Cu(0)–CO species reflects the different behaviors of the catalysts towards CO adsorption and reduction. The spectrum of Cu/TiO_2 exhibits an important and symmetric signal of CO bound to metallic copper centered at 2097 cm^{-1}. This feature is similar to that already observed for Cu/Al_2O_3, but the much stronger intensity and the shift to slightly lower energies revealed a higher reduction degree of the copper phase. For Cu/SiO_2 only a very weak signal was detected at about 2118 cm^{-1}, related to a more oxidized form of the copper constituent, *i.e.* Cu_2O. The temperature dependent behaviors of CO adsorption on Cu/TiO_2 and Cu/SiO_2 were comparable to that displayed by Cu/Al_2O_3 (not shown, see Fig. 1). The signal of CO adsorbed on Cu/TiO_2 was attenuated following the lowering of the adsorption temperature. The weak feature observed for Cu/SiO_2 at 353 K vanished at 283 K.

On the basis of this analysis, the propensity of the copper species to undergo spontaneous reduction depends on the support and follows the sequence $TiO_2 > Al_2O_3 > SiO_2$. Copper species on TiO_2 are reduced to the highest extent.

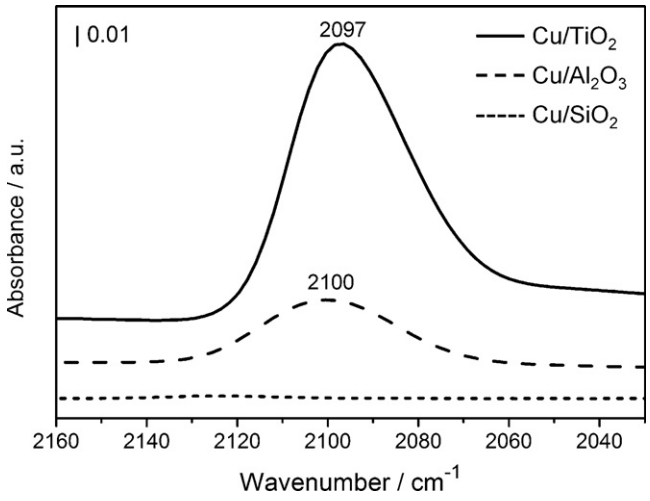

Fig. 2. ATR-IR spectra of CO adsorbed from heptane on pre-reduced Cu/Al_2O_3, Cu/TiO_2 and Cu/SiO_2. Conditions: heptane solvent, CO, 2 h, 353 K. Pre-reduction: 453 K. *In situ* reduction: 353 K.

3.3. DRIFTS

In order to compare the results obtained during CO adsorption from the liquid with corresponding measurements made in the gas phase, *in situ* DRIFT experiments were performed under similar conditions (reduction and adsorption temperatures) as used in the ATR-IR studies (Fig. 3). The DRIFT spectra collected on powder samples reduced in H_2 flow at 353 K and exposed to CO at the same temperature indicated that only Cu/TiO_2 produced a very strong signal for Cu(0)–CO at 2109 cm^{-1}. No CO adsorption occurred on Cu/Al_2O_3 and Cu/SiO_2 (Fig. 3a). Only when the activation temperature was increased to 453 K, CO adsorption was detected for all materials (Fig. 3b). Cu/TiO_2 showed again the most intense signal (2112 cm^{-1}). A less intense signal was detected at 2124 cm^{-1} for Cu/SiO_2 and an even weaker signal was observed for Cu/Al_2O_3 at 2106 cm^{-1}. The position of the CO signals for alumina- and titania-supported catalysts is similar, suggesting that metallic copper was produced on these supports. The significant difference in the intensity of the two signals indicates that reduction of copper on alumina is less favored and some copper could be trapped in the catalyst as less easily reducible copper aluminate [63]. This issue will be addressed in more detail along with the XAS analysis. The carbonyl signal on Cu/SiO_2 is centered at higher energies and indicates that mainly oxidized Cu species are present. All signals disappeared when changing the feed to pure Ar.

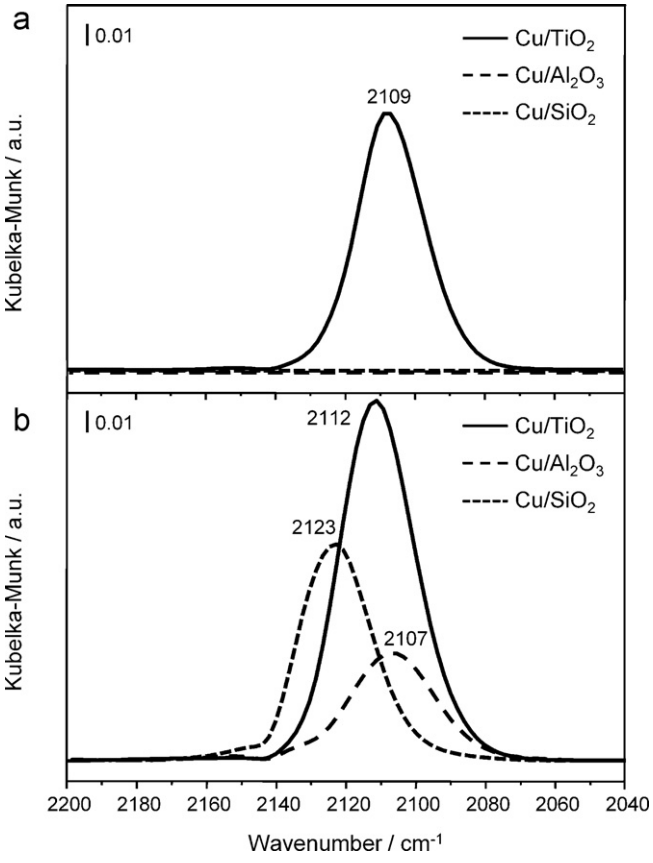

Fig. 3. DRIFTS spectra of CO adsorbed on Cu/TiO_2, Cu/Al_2O_3 and Cu/SiO_2 reduced at 353 K (a) and 453 K (b). Conditions: CO, 1 h, 353 K.

3.4. XAS

X-ray absorption spectroscopy in terms of X-ray absorption near edge structure (XANES) and extended X-ray absorption fine structure (EXAFS) was used to monitor the state of copper during both the gas phase reduction treatment and CO adsorption from the liquid phase, under experimental conditions similar to the ATR-IR investigations. Determination of the metal oxidation state was achieved by analysis of the near edge structure (white line at 8.979 keV) and the Fourier transformed EXAFS spectra at the Cu K edge (Cu–Cu and Cu–O scattering at 2.2 Å and 1.5 Å, respectively).

Before adsorption of the probe molecule, copper reduction in contact with a H_2/He gas mixture was followed from 298 K to 453 K for all the materials and up to 543 K for Cu/Al_2O_3 and Cu/SiO_2 (Fig. 4). Although the reduction degree was limited below temperatures of about 413 K, the sequences of XANES spectra acquired at higher temperatures evidenced marked differences between the supports, in terms of dynamics of the reduction process. The XANES spectra of Cu/TiO_2 (Fig. 4a) evidenced a fast decrease of the white line and an increase of the pre-edge region, indicating copper reduction. A steady-state was reached already after a few minutes at 453 K, indicating that reduction was complete. With Cu/SiO_2 (Fig. 4b), a significant degree of reduction was achieved after 30 min at 453 K, but a temperature up to 543 K was needed to obtain the spectral pattern typical of the fully reduced (metallic) copper species. This may be partially due to the higher dispersion and/or possible formation of copper silicates. The reduction kinetics was even slower for Cu/Al_2O_3 (Fig. 4c), the white line being only slightly diminished at 453 K and still appreciably intense up to 518 K. After 1 h at 543 K the copper nanoparticles on alumina were reduced as well. Nevertheless, the observed profiles allow suggesting the presence of additional copper species, such as copper aluminates, which are reduced only under more rigorous conditions [63–67]. In particular, the formation of such species is supported by the higher intensity of the white line [64] for Cu/Al_2O_3 with respect to those of Cu/TiO_2 and Cu/SiO_2. Moreover, no Cu–Cu contribution is detected in the FT-EXAFS spectra as in the case of Cu/TiO_2 (Fig. 5f, at *ca.* 3.8–4.1 Å), which leads to a lower reduction temperature than in highly dispersed systems or copper aluminates.

After gas phase reduction, Cu/Al_2O_3 and Cu/TiO_2 were cooled to 353 K under inert gas flow, shortly exposed to air (see Section 2.4) and then contacted with the H_2-saturated heptane for 1 h. CO adsorption from heptane was then performed. As in the ATR-IR measurements, the catalysts were later exposed to O_2-saturated and finally to CO-saturated solvent a second time. The XANES and Fourier transformed EXAFS spectra (FT-EXAFS) collected during the experiments are shown in Fig. 5.

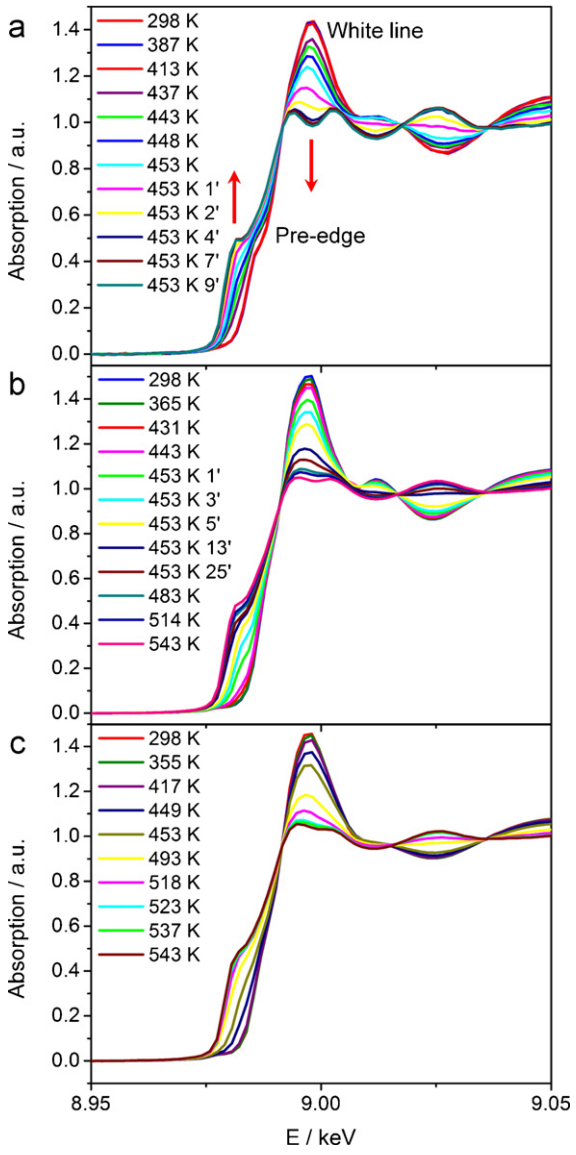

Fig. 4. XANES spectra collected during reduction under H_2/He flow for (a) Cu/TiO_2, (b) Cu/SiO_2 and (c) Cu/Al_2O_3. Conditions: 5 vol.% H_2/He, ramping the temperature from 298 K to 453 K (Cu/TiO_2) or 543 K and maintaining the final temperature for 1 h. (For interpretation of the references to color in this figure legend, the reader is referred to the web version of this article.)

For Cu/Al_2O_3 pre-reduced at 453 K (Fig. 5a and b) the oxidation state of copper did not substantially change upon contact with the H_2- and CO-saturated solvent. The intensity of the white line in the XANES spectra, as well as of the Cu–O contribution in the FT-EXAFS spectra, remained in fact substantially unperturbed. In an identical experiment with Cu/Al_2O_3 pre-reduced at 543 K (Fig. 5c and d) the short contact with air induced partial re-oxidation of copper. Accordingly, an increase of the white line intensity in the XANES spectrum and enhancement of the Cu–O scattering and lowering of the Cu–Cu scattering were observed in the spectra. Nevertheless, upon admission of the solvent saturated with the reducing gases the extent of reduction rose again in both environments (depletion of the Cu(I) component). The reduction degree achieved during the gas phase treatment was however not recovered. Subsequent contact with O_2 caused oxidation of the copper phase. Readmission of CO did not lead to further reduction. With Cu/TiO_2, the H_2-saturated solvent appeared to further reduce the copper phase, compared to the reduction degree achieved upon gas phase treatment. CO caused an additional increase of the content of metallic Cu (Fig. 5e and f), as indicated by higher intensity of the Cu–Cu contribution in the FT-EXAFS spectrum. Exposure to O_2-saturated solvent changed the oxidation state of copper in the same direction as for Cu/Al_2O_3, but in this case the Cu(0) peak still largely dominated the spectrum. The successive admission of CO-saturated solvent did not significantly modify the scenario to a remarkable extent.

3.5. Catalytic tests

Cu/Al_2O_3, Cu/TiO_2 and Cu/SiO_2 (pre-reduced at 543 K) have shown remarkable performance in the anaerobic oxidation of secondary, allylic, benzylic and steroid alcohols in the presence of a hydrogen acceptor [35,36]. In the test reaction, the oxidation of 3-octanol to 3-octanone in the presence of styrene as acceptor, all the supported copper catalysts virtually afforded 100% selectivity to the carbonyl compound. However, different conversions levels were observed. In order to correlate our characterization results with the catalytic behavior, we carried out the oxidation of 3-octanol in the absence of styrene and before the hydrogenation of the product intervenes (dehydrogenation conditions) [36,68]. Under these conditions, the catalyst activity was assumed to depend only on the dehydrogenation efficiency of the metal and the intrinsic properties of the support. Additionally, the temperature of the reductive pre-treatment was set at 413 K in order to take advantage of the different extent of copper reduction observed, thus enhancing the differences. The typical catalyst reduction at 543 K would in fact lead to a uniform and high reduction degree of copper for all catalysts. Fig. 6 shows the conversion of 3-octanol for the three materials after 30 min of reaction. The overall poor conversion values are an obvious consequence of the predominance of oxidized copper species on the catalyst surface due to the experimental conditions. However, reproducible differences in catalytic behavior were observed. The activities expressed as turnover frequencies (TOFs) at 10% 3-octanol conversion based on the surface area of exposed copper were 109 h^{-1} for $CuTiO_2$, 57 h^{-1} for Cu/Al_2O_3, and 17 h^{-1} for Cu/SiO_2 indicating that the activity decreases in the sequence $Cu/TiO_2 > Cu/Al_2O_3 > Cu/SiO_2$. Note that this order correlates with the degree of reduction of the differently supported copper constituent observed in the liquid phase. It should be stressed that a possible size effect of the significantly smaller Cu particles in Cu/SiO_2 on the reduction behavior and the catalytic activity cannot be ruled out.

4. Discussion

CO adsorption from the gas phase on supported Cu catalysts has been extensively used to characterize the state of the metal particles [55,56,58–62]. Our *in situ* ATR-IR and XAS investigations, monitoring the interaction of CO at the solvent–copper interface, disclose new aspects of the redox properties of these supported nanoparticles in their working state and provide valuable information on the role played by the nature of the support. The copper phase underwent spontaneous reduction to significant extent by CO in heptane at 353 K and some reduction was observed even at lower temperatures. This is not the first example in which solvent assisted conditions are able to strongly influence the temperature at which reduction occurs with respect to that in the gas phase. Similarly, palladium and platinum based catalysts were reduced in the presence of H_2 and cyclohexane at 323 K [51,69].

The nature of the support has been shown to have a strong influence on the redox properties of copper. The highest reduction extent was observed for Cu/TiO_2. The reduction of the copper constituent was rather easy for Cu/Al_2O_3 as well, but more difficult for Cu/SiO_2. The XAS analysis from the liquid phase indicates

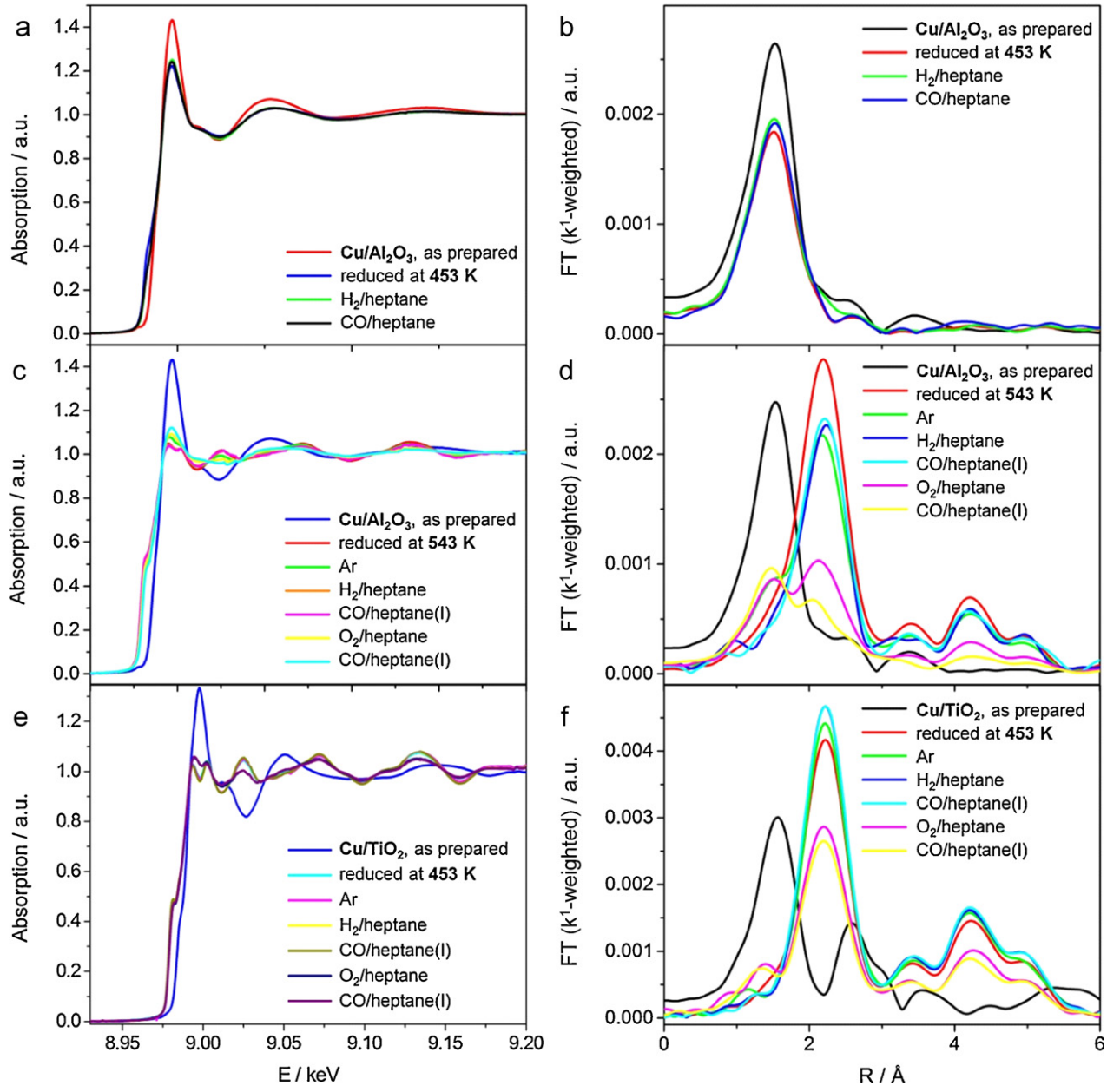

Fig. 5. XANES and Fourier transformed EXAFS spectra (not corrected for phase shift) collected during CO adsorption from the liquid phase for (a–d) Cu/Al_2O_3 and (e, f) Cu/TiO_2. Conditions: gas-phase reduction at 453 or 543 K, 5 vol.% H_2/He-saturated heptane (1 h), 10 vol.% CO/Ar-saturated heptane (1 h), 353 K. (For interpretation of the references to color in this figure legend, the reader is referred to the web version of this article.)

that a higher reduction extent was indeed achieved for Cu/TiO_2 and Cu/Al_2O_3 during contact with H_2-saturated heptane and upon CO adsorption with respect to the starting conditions (pre-reduction at 453 and 543 K, respectively), confirming the results of the infrared analysis and establishing a link between surface and bulk properties of the investigated systems. In the corresponding low temperature *in situ* DRIFT experiment, copper remained in almost totally oxidized state, besides for some more prominent reduction in the Cu/TiO_2 system. Only higher pre-reduction temperatures enabled significant copper reduction. The gas-phase infrared data are in line with the H_2-TPR data in the literature [36,55].

Further insight into the reduction process for the three catalysts was provided by gas phase XAS analysis. Copper constituents were indeed observed to fully reduce to metallic copper on titania with fast kinetics at 453 K, as a feasible consequence of the strong interaction with the support [70]. Note that the EXAFS spectra indicate here the existence of copper oxide nanoparticles due to a significant Cu backscattering which seem to lead to this easier reduction. The reduction process is slower for the alumina- and silica-supported catalysts. The detection of copper silicates and the higher Cu dispersion in Cu/SiO_2 as well as the formation of spinels in Cu/Al_2O_3 may explain the difficult reduction. Copper aluminates were already observed in similar systems [57,63,64]. Furthermore, time resolved XAS analysis of the redox properties of a Cu/Al_2O_3 catalyst in the subsecond time scale recently evidenced transient Cu(I) species as intermediate in redox processes [52,67].

The combined *in situ* approach evidenced a far higher reducibility of copper supported on alumina both with XAS and IR compared to that on silica. This finding well relates to the superior performance exhibited by the former catalyst in alcohol oxidation in terms of shorter reaction times and the required lower temperature pre-treatment [35]. It is indeed at low temperature where the catalysts offer more drastic differences of reduction extent of the metal nanostructures. The activity order $Cu/TiO_2 > Cu/Al_2O_3 > Cu/SiO_2$

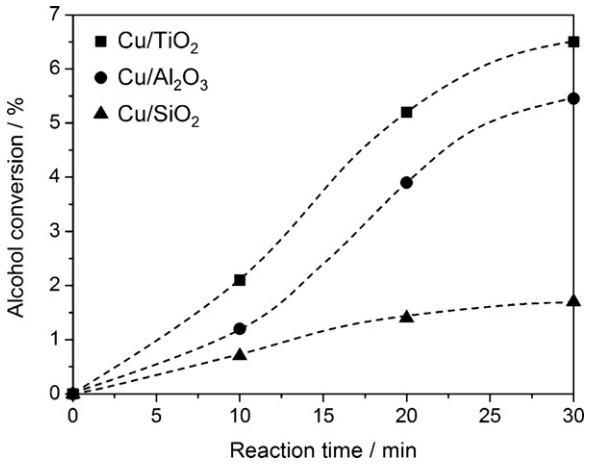

Fig. 6. Oxidation of 3-octanol to 3-octanone on Cu/Al_2O_3, Cu/TiO_2 and Cu/SiO_2 activated at 413 K. Conditions: 0.1 g catalyst pre-treated at 413 K, 0.1 g 3-octanol, 8 ml toluene, 363 K, N_2, 30 min.

shown for the oxidation of 3-octanol resembles the order of reducibility observed for copper constituents in the liquid phase, but not in the gas phase. This indicates that the redox behavior in the medium where the reaction occurs is relevant and that measuring the redox behavior in a different phase (gas phase) may not give a proper correlation between redox behavior and catalytic activity for the catalytic system investigated. The major difference between the reduction in the liquid and gas phase is the mass transfer. In the liquid phase diffusion of dihydrogen to the solid surface is much slower, giving rise to possible mass transfer control if the reduction is fast. Thus ideally for correlating the reduction behavior with catalytic activity, the reduction behavior should be studied in the same medium as the reaction is performed.

In spite of the fact that the redox behavior of the Cu nanoparticles seems to play a crucial role, it is likely not the only factor determining their activity in the test reaction studied. The acid–base properties of the support seem also to be crucial [57,71]. Discrimination between the effect of these properties and the role of the redox behavior of the supported Cu nanoparticles is a challenging task due to the interrelation of these properties. Further work will therefore be necessary to properly assign the role of these factors in the alcohol oxidation.

5. Conclusions

In situ ATR-IR and XAS have been applied to investigate the redox behavior of copper nanoparticles supported on Al_2O_3, TiO_2 and SiO_2 in the liquid and gas phase. The comparison with data obtained from conventional gas phase characterization reveals some differences in the redox behavior of Cu-based catalysts. The solvent (heptane) is shown to play an important role in lowering the temperature at which copper reduction occurs compared to reduction in gas-phase. Another crucial factor is the nature of the support leading to different extent of reduction under similar conditions. A higher reduction extent of the copper constituent is achieved on TiO_2 and Al_2O_3 in the liquid phase compared to that in the gas phase. The reduction behavior in the liquid phase well correlates with the catalytic activity of these catalysts in the liquid-phase dehydrogenation of 3-octanol. The study indicates that for correlating the redox behavior with catalytic activity, the former should be measured *in situ* in the same medium as used in the catalytic reaction. Redox behaviors measured in the gas phase may greatly differ from those determined in the liquid phase mainly due to much faster mass transfer (diffusion) compared to that in the liquid phase.

Acknowledgments

Financial support for this work was provided by the Foundation Claude and Giuliana. The authors thank ANKA (KIT, Karlsruhe, Germany) for providing beam time, Dr. Stefan Mangold and Dr. Matteo Caravati for support during the XAS measurements. Dr. Federica Zaccheria is acknowledged for the catalytic tests and fruitful discussions. C.M. received a scholarship from the University of Milan. The work at the synchrotron radiation sources was supported by the European Community-Research Infrastructure Action under the FP6 program, "Structuring the European Research Area" (through the Integrated Infrastructure Initiative "Integrating Activity on Synchrotron and Free Electron Laser Science," contract RII3-CT-2004-506008).

Appendix A. Supplementary data

Supplementary data associated with this article can be found, in the online version, at doi:10.1016/j.cattod.2011.08.043.

References

[1] N.R. Shiju, V.V. Guliants, Appl. Catal. A 356 (2009) 1–17.
[2] L.D. Pachon, G. Rothenberg, Appl. Organomet. Chem. 22 (2008) 288–299.
[3] R.J. White, R. Luque, V.L. Budarin, J.H. Clark, D.J. Macquarrie, Chem. Soc. Rev. 38 (2009) 481–494.
[4] V. Polshettiwar, R.S. Varma, Green Chem. 12 (2010) 743–754.
[5] G.L. Haller, D.E. Resasco, Adv. Catal. 36 (1989) 173–235, and references therein.
[6] M.S. Wainwright, D.L. Trimm, Catal. Today 23 (1995) 29–42, and references therein.
[7] Y. Okamoto, K. Fukino, T. Imanaka, S. Teranishi, J. Phys. Chem. 87 (1983) 3747–3754.
[8] M.G. Sanchez, J.L. Gazquez, J. Catal. 104 (1987) 120–135.
[9] E.I. Solomon, P.M. Jones, J.A. May, Chem. Rev. 93 (1993) 2623–2644.
[10] B.R. Cuenya, Thin Solid Films 518 (2010) 3127–3150.
[11] X.M. Liu, G.Q. Lu, Z.F. Yan, J. Beltramini, Ind. Eng. Chem. Res. 42 (2003) 6518–6530.
[12] N. Takezawa, N. Iwasa, Catal. Today 36 (1997) 45–56.
[13] J. Agrell, H. Birgersson, M. Boutonnet, I. Melian-Cabrera, R.M. Navarro, J.L.G. Fierro, J. Catal. 219 (2003) 389–403.
[14] C. Lamberti, C. Prestipino, F. Bonino, L. Capello, S. Bordiga, G. Spoto, A. Zecchina, S.D. Moreno, B. Cremaschi, M. Garilli, A. Marsella, D. Carmello, S. Vidotto, G. Leofanti, Angew. Chem. Int. Ed. 41 (2002) 2341–2344.
[15] H. Yahiro, M. Iwamoto, Appl. Catal. A 222 (2001) 163–181.
[16] S. Bennici, A. Gervasini, N. Ravasio, F. Zaccheria, J. Phys. Chem. B 107 (2003) 5168–5176.
[17] C. Kiener, M. Kurtz, H. Wilmer, C. Hoffmann, H.W. Schmidt, J.-D. Grunwaldt, M. Muhler, F. Schuth, J. Catal. 216 (2003) 110–119.
[18] H. Praliaud, S. Mikhailenko, Z. Chajar, M. Primet, Appl. Catal. B 16 (1998) 359–374.
[19] V. Indovina, M. Occhiuzzi, D. Pietrogiacomi, S. Tuti, J. Phys. Chem. B 103 (1999) 9967–9977.
[20] C. Marquez-Alvarez, I. Rodrıguez-Ramos, A. Guerrero-Ruiz, G.L. Haller, M. Fernandez-Garcıa, J. Am. Chem. Soc. 119 (1997) 2905.
[21] J.-D. Grunwaldt, A.M. Molenbroek, N.Y. Topsøe, H. Topsøe, B.S. Clausen, J. Catal. 194 (2000) 452–460.
[22] B. Berthon, A. Forestiere, G. Leleu, B. Sillion, Tetrahedron Lett. 22 (1981) 4073–4076.
[23] T. Yamakawa, T. Ohnishi, S. Shinoda, Catal. Lett. 23 (1994) 395–401.
[24] N. Ravasio, M. Antenori, M. Gargano, M. Rossi, J. Mol. Catal. (1992) 267–274.
[25] N. Ravasio, M. Gargano, M. Rossi, J. Org. Chem. 58 (1993) 1259–1261.
[26] N. Ravasio, N. Poli, R. Psaro, M. Saba, F. Zaccheria, Top. Catal. (2000) 195–199.
[27] A.J. Marchi, D.A. Gordo, A.F. Trasarti, C.R. Apesteguia, Appl. Catal. A 249 (2003) 53–67.
[28] T. Yamakawa, I. Tsuchiya, D. Mitsuzuka, T. Ogawa, Catal. Commun. 5 (2004) 291–295.
[29] N. Ravasio, F. Zaccheria, P. Allegrini, M. Ercoli, Catal. Today 121 (2007) 2–5.
[30] X.Y. Liu, R.J. Madix, C.M. Friend, Chem. Soc. Rev. 37 (2008) 2243–2261.
[31] K. Yoshida, C. Gonzalez-Arellano, R. Luque, P.L. Gai, Appl. Catal. A 379 (2010) 38–44.
[32] T. Turek, D.L. Trimm, Catal. Rev. Sci. Eng. 36 (1994) 645–683.
[33] A. Baiker, J. Kijenski, Catal. Rev. Sci. Eng. 27 (1985) 653–697.
[34] V. di Castro, M. Gargano, N. Ravasio, M. Rossi, in: G. Poncelet, P.A. Jacobs, P. Grange, B. Delmon (Eds.), Stud. Surf. Sci. Catal., Elsevier, Amsterdam, 1991, p. 95.
[35] F. Zaccheria, N. Ravasio, R. Psaro, A. Fusi, Chem. Commun. (2005) 253–255.
[36] F. Zaccheria, N. Ravasio, R. Psaro, A. Fusi, Chem. Eur. J. 12 (2006) 6426–6431.
[37] J.S. Bradley, J.M. Millar, E.W. Hill, C. Klein, B. Chaudret, A. Duteuil, J.W. Geus, R.W. Joyner, P. Fouilloux, P.A. Sermon, M. Ichikawa, F. Bozonverduraz, Stud. Surf. Sci. Catal. 75 (1993) 969–979.

[38] C. Keresszegi, D. Ferri, T. Mallat, A. Baiker, J. Phys. Chem. B 109 (2005) 958–967.
[39] C. Mondelli, D. Ferri, J.-D. Grunwaldt, F. Krumeich, S. Mangold, R. Psaro, A. Baiker, J. Catal. 252 (2007) 77–87.
[40] T. Mallat, E. Orglmeister, A. Baiker, Chem. Rev. 107 (2007) 4863–4890.
[41] S.D. Ebbesen, B.L. Mojet, L. Lefferts, Langmuir 24 (2008) 869–879.
[42] D. Ferri, A. Baiker, Top. Catal. 52 (2009) 1323–1333.
[43] C. Mondelli, J.-D. Grunwaldt, D. Ferri, A. Baiker, Phys. Chem. Chem. Phys. 12 (2010) 5307–5316.
[44] P. Haider, B. Kimmerle, F. Krumeich, W. Kleist, J.-D. Grunwaldt, A. Baiker, Catal. Lett. 125 (2008) 169–176.
[45] M. Caravati, J.-D. Grunwaldt, A. Baiker, Catal. Today 126 (2007) 27–36.
[46] J. Sa, C. Kartusch, M. Makosch, C. Paun, J.A. van Bokhoven, E. Kleymenov, J. Szlachetko, M. Nachtegaal, H.G. Manyar, C. Hardacre, Chem. Commun. 47 (2011) 6590–6592.
[47] G.M. Hamminga, G. Mul, J.A. Moulijn, Chem. Eng. Sci. 59 (2004) 5479–5485.
[48] M.K. Schröter, L. Khodeir, J. Hambrock, E. Löffler, M. Muhler, R.A. Fischer, Langmuir 20 (2004) 9453–9455.
[49] T. Hikov, M.K. Schröter, L. Khodeir, A. Chemseddine, M. Muhler, R.A. Fischer, Phys. Chem. Chem. Phys. 8 (2006) 1550–1555.
[50] J.S. Bradley, E.W. Hill, B. Chaudret, A. Duteil, Langmuir 11 (1995) 693–695.
[51] T. Bürgi, R. Wirz, A. Baiker, J. Phys. Chem. B 107 (2003) 6774–6781.
[52] J.-D. Grunwaldt, M. Caravati, S. Hannemann, A. Baiker, Phys. Chem. Chem. Phys. 6 (2004) 3037–3047.
[53] C. Keresszegi, J.-D. Grunwaldt, T. Mallat, A. Baiker, J. Catal. 222 (2004) 268–280.
[54] T. Ressler, J. Synchrotron Radiat. 5 (1998) 118–122.
[55] F. Boccuzzi, A. Chiorino, G. Martra, M. Gargano, N. Ravasio, B. Carrozzini, J. Catal. 165 (1997) 129–139.
[56] F. Boccuzzi, S. Coluccia, G. Martra, N. Ravasio, J. Catal. 184 (1999) 316–326.
[57] A. Gervasini, M. Manzoli, G. Martra, A. Ponti, N. Ravasio, L. Sordelli, F. Zaccheria, J. Phys. Chem. B 110 (2006) 7851–7861.
[58] K.I. Hadjiivanov, G.N. Vayssilov, Adv. Catal. (2002) 307–511.
[59] M.B. Padley, C.H. Rochester, G.J. Hutchings, F. King, J. Catal. 148 (1994) 438–452.
[60] A. Dandekar, M.A. Vannice, J. Catal. 178 (1998) 621–639.
[61] S. Zeradine, A. Bourane, D. Bianchi, J. Phys. Chem. B 105 (2001) 7254–7257.
[62] O. Dulaurent, X. Courtois, V. Perrichon, D. Bianchi, J. Phys. Chem. B 104 (2000) 6001–6011.
[63] P. Kappen, J.-D. Grunwaldt, B.S. Hammershoi, L. Troger, B.S. Clausen, J. Catal. 198 (2001) 56–65.
[64] C. Prestipino, S. Bordiga, C. Lamberti, S. Vidotto, M. Garilli, B. Cremaschi, A. Marsella, G. Leofanti, P. Fisicaro, G. Spoto, A. Zecchina, J. Phys. Chem. B 107 (2003) 5022–5030.
[65] J.-D. Grunwaldt, C. Kiener, F. Schuth, A. Baiker, Phys. Scripta T115 (2005) 819–821, and references therein.
[66] J.-D. Grunwaldt, B. Kimmerle, S. Hannemann, A. Baiker, P. Boye, C.G. Schroer, J. Mater. Chem. 17 (2007) 2603–2606.
[67] J. Stötzel, D. Lützenkirchen-Hecht, R. Frahm, B. Kimmerle, A. Baiker, M. Nachtegaal, M.J. Beier, J.-D. Grunwaldt, J. Phys.: Conf. Ser. 190 (2009) 012153.
[68] F. Zaccheria, A. Fusi, R. Psaro, N. Ravasio, in: J. Sowa (Ed.), Chemical Industries Series (Catalysis of Organic Reactions), Taylor and Francis, Boca Raton, 2005, p. 293.
[69] D. Ferri, T. Bürgi, A. Baiker, J. Phys. Chem. B 105 (2001) 3187–3195.
[70] P. Weerachawanasak, P. Praserthdam, M. Arai, J. Panpranot, J. Mol. Catal. A 279 (2008) 133–139.
[71] H. Lauron-Pernot, Catal. Rev. Sci. Eng. 48 (2006) 315–361.